J. Nonlinear Var. Anal. 6 (2022), No. 6, pp. 675-691
Available online at http://jnva.biemdas.com
https://doi.org/10.23952/jnva.6.2022.6.06

A TRUST-REGION INTERIOR-POINT TECHNIQUE TO SOLVE MULTI-OBJECTIVE OPTIMIZATION PROBLEMS AND ITS APPLICATION TO A TUBERCULOSIS OPTIMAL CONTROL PROBLEM

JAUNY[1], DEBDAS GHOSH[1], ASHUTOSH UPADHAYAY[1], QAMRUL HASAN ANSARI[2,*]

[1]*Department of Mathematical Sciences, Indian Institute of Technology (BHU), Varanasi 221 005, India*
[2]*Department of Mathematics, Aligarh Muslim University, Aligarh 202 002, India*

Abstract. We introduce a trust-region interior-point technique to generate the Pareto optimal solution for multi-objective optimization problems. The Pascoletti-Serafini scalarization technique is utilized to convert a multi-objective optimization problem into a set of single-objective optimization subproblems. Then, the subproblems are solved by a trust-region interior-point method. Using the sequential quadratic programming technique, the algorithm proceeds through a sequence of barrier problems. With the help of the stationary points of a merit function, we obtain stationary points of the objective function of the barrier problem. It is shown that the directions that are used to find the sequence of iterates of the proposed method are descent direction of the used merit function. To show the efficiency of the proposed method, we show its performance on some standard test problems. As an application, we apply the proposed algorithm to solve an optimal control problem for a tuberculosis model. The model problem is a minimization problem and it has two objectives: one is the sum of the active infections patient and persistent latent individual, and the other is the cost to implement the control strategies.

Keywords. Interior-point method; Multi-objective optimization; Optimal control theory; Trust region; Tuberculosis.

1. Introduction

Real-world optimization problems (see, e.g., [1, 2, 3, 4, 5]) often involve two or more objectives simultaneously. Therefore, the identification and characterization of solutions to multi-objective optimization problems (MOPs) have become a very important task. MOPs attempt to optimize several conflicting objectives simultaneously. Consequently, efficiency, weak efficiency, strict efficiency, and proper efficiency (see [6, 7]) are commonly used to characterize the relative optimal decisions.

Scalarization techniques [8] have been popular methods to study MOPs. Pascoletti-Serafini [9] proposed a scalar optimization problem for determining (weakly) efficient solutions of a given MOP in terms of a given ordering cone. Compared with other existing scalarization techniques [8], these methods have many advantages including handling nonconvexity [10]. In addition, some popular scalarization techniques such as weighted sum [11, 12], ε-constraint [13], normal boundary intersection [14], ideal cone [15], etc. can be obtained by selecting suitable values of parameters and choosing an ordering cone. Recently, a modified Pascoletti-Serafini scalarization technique [16] has been established to generate the (weakly and properly) efficient solutions of the MOPs. Generally, the nature

*Corresponding author.
E-mail addresses: debdas.mat@iitbhu.ac.in (D. Ghosh), jauny.rs.mat17@itbhu.ac.in (Jauny), qhansari@gmail.com (Q.H. Ansari), ashutosh.upadhayay.rs.mat18@itbhu.ac.in (A. Upadhayay).
Received December 23, 2021; Accepted April 10, 2022.

of converted scalar optimization problem by modified Pascoletti-Serafini scalarization technique is nonconvex. Therefore, this scalar optimization problem is hard to solve. Thus, we adopt an interior-point method with a trust region strategy to tackle the scalar optimization problem.

Until Karmarkar [17] proposed a polynomial-time method to solve linear programming problems, the simplex method was the only viable one. In contrast to the exponential complexity of the simplex method, Karmarkar's algorithm has polynomial complexity. Since the interior-point algorithm successfully solves linear programming problems, researchers have attempted to implement linearization methodologies for solving nonlinear programming problems. In this study, a penalty method along with a barrier method is used to convert a constrained nonlinear programming problem into an unconstrained problem. Newton method is applied to the barrier Karush–Kuhn–Tucker conditions. The benefit of Newton method is that it converges quadratically to a stationary point. Still, its downside is that the starting point must be sufficiently close to the stationary point to assure the convergence. To ensure the convergence from any starting point, the trust-region approach [18, 19] is proven successful for a single-objective unconstrained and constrained optimization problems.

In this paper, we apply the trust-region strategy along with the interior-point method for solving transformed scalar optimization subproblems. It does not require the objective function of the model to be convex. Additionally, it does not require the Hessian of the objective function to be positive definite. To show the applicability of the proposed method, we apply it some standard test problems and a multi-objective optimal control problem that governs the dynamics of tuberculosis, as suggested in [20]. We propose a multi-objective approach to find the optimal control strategies. The approach reflects the intrinsic nature of an underlying decision-making problem. It avoids the use of additional parameters needed to formulate the cost functional and allows to obtain the whole range of optimal solutions. We also investigate the effect of different values of transmission coefficient on optimal solutions.

This paper is structured as follows. In Section 2, we provide the required terminologies and notations. In Section 3, a brief overview is described of modified Pascoletti and Serafini scalarization technique. The methodology of solving the converted scalar problem by interior point with trust region strategy is described in section 4. Section 5 shows the results obtain by applying the proposed method over some commonly used test problems. Section 6 displays the results which concerns with the application of the proposed method on a multi-objective optimal control problem for tuberculosis. Finally, Section 7 ends with the concluding remarks.

2. Basic Ideas and Preliminaries

The mathematical description of a multi-objective optimization problem is as follows:

$$\left.\begin{array}{c}\text{minimize } f(x) = (f_1(x), f_2(x), \ldots, f_p(x))^\top,\ p \geq 2\\ \text{subject to } x \in \mathscr{X},\end{array}\right\} \tag{2.1}$$

where $x = (x_1, x_2, \ldots, x_n)^\top$ denotes the n-dimensional decision vector in the decision space $\mathscr{X} = \{x \in \mathbb{R}^n : h_i(x) \geq 0,\ i = 1,2,\ldots,m,\ x \geq 0\}$, $f(x)$ denotes the objective vector containing p conflicting functions to be minimized, and $h_i : \mathbb{R}^n \to \mathbb{R}$ are twice continuously differentiable functions for all $j = 1,2,\ldots,p$ and $i = 1,2,\ldots,m$. We denote the image of $\mathscr{X}$ under the vector-valued objective function f by $\mathscr{Y}$, i.e.,

$$\mathscr{Y} = f(\mathscr{X}) = \left\{(f_1(x), f_2(x), \ldots, f_p(x))^\top : x \in \mathscr{X}\right\}.$$

The set $\mathscr{Y}$ is referred to as the feasible set in objective space. Note that $\mathscr{X}$ is a subset of $\mathbb{R}^n$ and $\mathscr{Y}$ is a subset of $\mathbb{R}^p$.

Definition 2.1. (*Dominance* [7]). For any two vectors $x \in \mathscr{X}$ and $y \in \mathscr{X}$, x is said to dominate y, denoted as $f(x) \prec f(y)$ if $f_i(x) \leq f_i(y)$ for all $i = 1, 2, \ldots, p$ and $f_j(x) < f_j(y)$ for at least one $j = 1, 2, \ldots, p$. Also, x is said to be nondominated with y if x does not dominate y.

Definition 2.2. (*Pareto optimality* [7]). A point $\hat{x} \in \mathscr{X}$ is called efficient or Pareto optimal to the problem (2.1) if there is no other $x \in \mathscr{X}$ such that $f(x) \leq f(\hat{x})$. If $\hat{x}$ is efficient, then $f(\hat{x})$ is called a nondominated point.

The collection of all efficient points of the MOP (2.1) is denoted by $\mathscr{X}_E$. The set of all nondominated points is represented by $\mathscr{Y}_N$. Evidently, $\mathscr{Y}_N = f(\mathscr{X}_E)$. Generally, $\mathscr{Y}_N$ contains a large number of points. Therefore, practically, it is estimated by a sufficiently large and diverse set of representative points.

Definition 2.3. (*Weak Pareto optimality* [7]). A feasible solution $\hat{x} \in \mathscr{X}$ is called weakly efficient or weakly Pareto optimal if there is no $x \in \mathscr{X}$ such that $f(x) < f(\hat{x})$. The point $\hat{y} = f(\hat{x})$ is then said to be weakly nondominated.

The set of all weakly efficient solutions of the MOP (2.1) is denoted by $\mathscr{X}_{wE}$. The collection of all weakly nondominated points is represented by $\mathscr{Y}_{wN}$.

We use the following notations throughout the paper:

- $\mathbb{R}^p_{\geqq} = \{y \in \mathbb{R}^p : y \geq 0\}$, the nonnegative orthant of $\mathbb{R}^p_{\geqq}$.
- $\mathbb{R}^p_{\geq} = \{y \in \mathbb{R}^p : y \geq 0\}$, where $y \geq 0$ denotes $y \geqq 0$ but $y \neq 0$.
- $\mathbb{R}^p_{>} = \{y \in \mathbb{R}^p : y > 0\}$ represents the interior of $\mathbb{R}^p_{\geqq}$, where $y > 0$ means $y_i > 0$ for all $i = 1, 2, \ldots, p$.
- $\|x\| = \left(\sum_{i=1}^{n} |x_i|^2 \right)^{\frac{1}{2}}$.

In the next section, we present a scalarization technique which transforms the MOP (2.1) into a set of scalar optimization problems.

3. Pascoletti-Serafini Scalarization Technique

In this section, a brief review of the modified Pascoletti-Serafini scalarization technique [16] is introduced. Let $a \in \mathbb{R}^p_{\geqq}$ and $r \in \mathbb{R}^p_{\geqq} - \{0\}$. Then, the set of single objective nonlinear optimization subproblems, to solve (2.1), obtained by using the modified Pascoletti-Serafini scalarization technique is as follows:

$$\left.\begin{array}{ll} \text{minimize} & t - \omega^\top \theta \\ \text{subject to} & a + tr - f(x) - \theta \geq 0, \\ & h_i(x) \geq 0, \ i = 1, 2, \ldots, m, \\ & t \in \mathbb{R}, \ x \geq 0, \ \theta \geq 0, \end{array}\right\} \tag{3.1}$$

where $\omega_i \geq 0, \ i = 1, 2, \ldots, p$ are weights.

To obtained the (weakly) efficient solutions of MOP (2.1), Pascoletti and Serafini suggested to solve the transformed scalar optimization problem (3.1) by changing the values of the parameters $a \in \mathbb{R}^p_{\geqq}$, $r \in \mathbb{R}^p_{\geqq} - \{0\}$ and $\omega \geqq 0$.

We reformulate the problem (3.1) by introducing some notations. Let $c = (0, 0, \ldots, 0, 1, -1)^\top \in \mathbb{R}^{n+2}$, $\mathrm{x} = (x_1, x_2, \ldots, x_n, x_{n+1}, x_{n+2})^\top$, $h(\mathrm{x}) = \left(h_1(\mathrm{x}), h_2(\mathrm{x}), \ldots, h_m(\mathrm{x}), c^\top \mathrm{x}\right)^\top$, and $t = x_{n+1} - x_{n+2} = c^\top \mathrm{x}$. Then, problem (3.1) becomes

$$\left.\begin{aligned} &\text{minimize} && c^\top \mathrm{x} - \omega^\top \theta \\ &\text{subject to} && a + rc^\top \mathrm{x} - f(\mathrm{x}) - \theta \geq 0 \\ & && h(\mathrm{x}) \geq 0 \\ & && \mathrm{x} \geq 0,\ \theta \geq 0. \end{aligned}\right\} \tag{3.2}$$

We convert the inequality constraints of the problem (3.2) by introducing slack variables. Then, problem (3.2) can be rewritten as follows:

$$\left.\begin{aligned} &\text{minimize} && c^\top \mathrm{x} - \omega^\top \theta \\ &\text{subject to} && g(\mathrm{x},\theta) - s = 0 \\ & && s \geq 0, \end{aligned}\right\} \tag{3.3}$$

where $g(\mathrm{x},\theta) = \left(a + rc^\top \mathrm{x} - f(\mathrm{x}) - \theta, h(\mathrm{x}), \mathrm{x}, \theta\right)^\top$ and $s \in \mathbb{R}^{p+(m+1)+(n+2)+p}$ is the slack variable.

In the forthcoming section, the procedure of solving the scalar optimization problem (3.3) by using an interior-point method is derived. Since the nature of the problem (3.3) is nonconvex, a variant of interior point method is used to solve problem (3.3)

4. Interior-point Method with Trust-Region Strategy

In this section, scalar optimization problem (3.3) is solved with the help of an interior-point method with trust-region strategy. To make problem (3.3) more straightforward, we introduce a new variable $\mathrm{z} = (\mathrm{x},\theta)$. Now, we can rewrite problem (3.3) as follows:

$$\left.\begin{aligned} &\text{minimize} && \mathrm{F}(\mathrm{z}) = c^\top \mathrm{x} - \omega^\top \theta \\ &\text{subject to} && g(\mathrm{z}) - s = 0 \\ & && s \geq 0. \end{aligned}\right\} \tag{4.1}$$

For a given $\mu > 0$, a barrier problem associated to problem (4.1) is as follows:

$$\left.\begin{aligned} &\text{minimize} && \mathscr{B}(\mathrm{z},s;\mu) = \mathrm{F}(\mathrm{z}) - \mu \left(\sum_{i=1}^{n+2p+m+3} \log s_i \right) \\ &\text{subject to} && g(\mathrm{z}) - s = 0. \end{aligned}\right\} \tag{4.2}$$

The Lagrangian function associated with the barrier problem (4.2) is defined by

$$\mathscr{L}(\mathrm{z},s,y;\mu) = \mathscr{B}(\mathrm{z},s;\mu) + y^\top (g(\mathrm{z}) - s), \tag{4.3}$$

where $y \in \mathbb{R}^{p+(m+1)+(n+2)+p}$ is the Lagrange multiplier.

A sequential quadratic programming (SQP) method [21] with trust regions can solve the barrier problem (4.2) since it is an equality-constrained optimization problem. If SQP methods are directly applied to the barrier problem, they often produce very small step sizes that violate either or both of the positivity of the slack variables and the trust-region constraint. In order to address this issue, we design an SQP method that is tailored specifically to the structure of barrier problems.

We now apply the sequential quadratic programming method of [21] to barrier problem (4.2). For a given barrier parameter $\mu > 0$, at an iterate (z,s), we first compute the Lagrange multiplier y (see Section 4.2) and then compute a step $d = (d_{\mathrm{z}}, d_s)^\top$ by solving the following quadratic programming problem:

$$\left.\begin{aligned} \text{minimize} \quad & \nabla \mathrm{F}^\top d_\mathrm{Z} + \frac{1}{2} d_\mathrm{Z}^\top \nabla^2_{\mathrm{ZZ}} \mathscr{L} d_\mathrm{Z} - \mu e^\top S^{-1} d_s + \frac{1}{2} d_s^\top \Sigma d_s \\ \text{subject to} \quad & A(\mathrm{Z})^\top d_\mathrm{Z} - d_s + g(\mathrm{Z}) - s = \wp, \\ & \|(d_\mathrm{Z}, S^{-1} d_s)\| \leq \Delta, \\ & d_s \geq -\tau s, \end{aligned}\right\} \tag{4.4}$$

where S is the diagonal matrix whose diagonal entries are components of the vector s; the scalar $\tau \in (0,1)$ is chosen close to 1 (for example, 0.99); $A(\mathrm{Z})$ is the Jacobian of the function g and $\Sigma = \mu S^{-2}$; $\wp$ is the relaxation vector. The constraints $d_s \geq -\tau s$ maintain the positivity of d_s and the trust-region constraint $\|(d_\mathrm{Z}, S^{-1} d_s)\| \leq \Delta$ guarantees that the problem (4.4) has a finite solution even when $\nabla^2_{\mathrm{ZZ}} \mathscr{L}(\mathrm{Z}, s, y)$ is not positive definite. Therefore, the Hessian $\nabla^2_{\mathrm{ZZ}} \mathscr{L}(\mathrm{Z}, s, y)$ need never be modified. In addition, the trust-region formulation ensures that adequate progress is made at every iteration. To justify the scaling S^{-1} that is used in the constraints of problem (4.4), we note that the shape of the trust region must take into account the requirement that the slacks not approach to zero prematurely. The scaling S^{-1} serves this purpose because it restricts those components i of the step vector d_s for which s_i is close to its lower bound zero. In the next subsection, we provide the technique to compute the step d.

4.1. **Step computation.** Problem (4.4) is difficult to minimize exactly because of the presence of the nonlinear constraint $\|(d_\mathrm{Z}, S^{-1} d_s)\| \leq \Delta$ and the bounds $d_s \geq -\tau s$. An important observation is that we can compute useful inexact solutions, at moderate cost. Since this approach scales up well with the number of variables and constraints, it provides a framework for developing practical interior-point methods for large-scale optimization.

The first step in the solution process is to make a change of variables that transforms the trust-region constraint $\|(d_\mathrm{Z}, S^{-1} d_s)\| \leq \Delta$ into a ball. By defining

$$\tilde{d} = \begin{bmatrix} d_\mathrm{Z} \\ \tilde{d}_s \end{bmatrix} = \begin{bmatrix} d_\mathrm{Z} \\ S^{-1} d_s \end{bmatrix}, \tag{4.5}$$

we can now write problem (4.4) as follows:

$$\left.\begin{aligned} \text{minimize} \quad & \nabla \mathrm{F}^\top d_\mathrm{Z} + \frac{1}{2} d_\mathrm{Z}^\top \nabla^2_{\mathrm{ZZ}} \mathscr{L} d_\mathrm{Z} - \mu e^\top \tilde{d}_s + \frac{1}{2} \tilde{d}_s^{\top} S \Sigma S \tilde{d}_s \\ \text{subject to} \quad & A(\mathrm{Z})^\top d_\mathrm{Z} - S\tilde{d}_s + g(\mathrm{Z}) - s = \wp, \\ & \|(d_\mathrm{Z}, \tilde{d}_s)\| \leq \Delta, \\ & \tilde{d}_s \geq -\tau e. \end{aligned}\right\} \tag{4.6}$$

The choice of the relaxation vector $\wp$ requires careful consideration as it impacts the efficiency of the method. Our goal is to choose $\wp$ as the smallest vector such that the constraints $A(\mathrm{Z})^\top d_\mathrm{Z} - S\tilde{d}_s + g(\mathrm{Z}) - s = \wp$, $\|(d_\mathrm{Z}, \tilde{d}_s)\| \leq \Delta$ and $\tilde{d}_s \geq -\tau e$ are consistent for some reduced value of trust-region radius Δ. To compute the vector $\wp$, we solve the following problem in the variable $v = (v_\mathrm{Z}, v_s)$:

$$\left.\begin{aligned} \text{minimize} \quad & \|A(w)^\top d_\mathrm{Z} - S\tilde{d}_s + g(\mathrm{Z}) - s\|^2 \\ \text{subject to} \quad & \|(v_\mathrm{Z}, v_s)\| \leq 0.8\Delta, \\ & v_s \geq -(\tau/2)e. \end{aligned}\right\} \tag{4.7}$$

If we ignore the bound constraint $v_s \geq -(\tau/2)e$, this problem has the standard form of a trust-region problem [22], and we can compute an approximate solution by using the dogleg method [23]. If the solution violates the bounds $v_s \geq -(\tau/2)e$, we can reduce Δ so that these bounds are satisfied. After solving (4.7), we define the residuals $\wp$ as

$$\wp = A(\mathrm{z})^\top d_\mathrm{z} - S\tilde{d}_s + g(\mathrm{z}) - s. \tag{4.8}$$

We are now ready to compute an approximate solution $\tilde{d}$ of the problem (4.6). By (4.8), the vector v is a particular solution of the linear constraints in problem (4.7). We can then solve the problem (4.6) by using the projected conjugate gradient (CG) [24]. We terminate the projected CG iteration by Steihaug's rules [24]: During the solution by CG we monitor the satisfaction of the trust-region constraint $\|(d_\mathrm{z}, \tilde{d}_s)\| \leq \Delta$ and stop if the boundary of this region is reached, if negative curvature is detected, or if an approximation solution is obtained. If the solution given by the projected CG iteration does not satisfy the bound constraints $\tilde{d}_s \geq -\tau e$, we backtrack so that they are satisfied. After the step $(d_\mathrm{z}, \tilde{d}_s)$ has been computed, we recover d from (4.5).

4.2. **Choice of Lagrange multipliers and merit function.** At every iteration, the choice of Lagrange multiplier y remains positive. Therefore, at an iterate (z, s), we choose y as

$$y = \min\left\{10^{-3}, \frac{\mu}{s_i}\right\}. \tag{4.9}$$

This choice of Lagrange multiplier y which is obtained in this manner will always be positive.

The role of the merit function is to decide whether a step is productive and should be accepted. Since interior-point methods can be seen as methods for solving the barrier problem (4.2), it is appropriate to define the merit function ϕ in terms of barrier functions. We may use, for example, an exact merit function of the form

$$\phi_\nu(\mathrm{z}, s) = \mathscr{B}(\mathrm{z}, s; \mu) + \nu\|g(\mathrm{z}) - s\|, \tag{4.10}$$

where $\nu > 0$ is the penalty parameter.

The following theorem addresses the stationarity property of the merit function (4.10).

Theorem 4.1. *Consider barrier problem (4.2). For $\mu > 0$, let the point $\bar{\lambda}_\mu = (\bar{\mathrm{z}}_\mu, \bar{s}_\mu)$ be such that $g(\bar{\mathrm{z}}_\mu) - \bar{s}_\mu = 0$. Also, suppose the point $\bar{\lambda}_\mu$ is a stationary point of the merit function $\phi_\nu(\mathrm{z}, s)$. Then, the point $\bar{\lambda}_\mu$ is also a stationary point for the barrier function $\mathscr{B}$.*

Proof. The directional derivative of the merit function ϕ_ν at the point $\lambda_\mu = (\mathrm{z}_\mu, s_\mu)$ along the direction d is given by the following relation:

$$\left(\nabla\phi_\nu(\lambda_\mu)\right)^\top d = \left(\nabla\mathscr{B}(\lambda_\mu)\right)^\top d - \nu\|g(\mathrm{z}_\mu) - s_\mu\|. \tag{4.11}$$

For any $\mu > 0$, $\|g(\bar{\mathrm{z}}_\mu) - \bar{s}_\mu\| = 0$ and $\left(\nabla\phi_\nu(\bar{\lambda}_\mu)\right)^\top d = 0$. Then, from (4.11), we obtain $\left(\nabla\mathscr{B}(\bar{\lambda}_\mu)\right)^\top d = 0$. Hence, $\bar{\lambda}_\mu$ is the stationary point for the barrier function. □

In trust-region methods, the step d is valid if the following inequality holds:

$$\frac{\mathrm{pred}(d)}{\mathrm{ared}(d)} \leq \eta, \tag{4.12}$$

where $\eta > 0$, the *actual reduction* (ared) is defined as

$$\mathrm{ared}(d) = \phi_\nu(\mathrm{z}, s) - \phi_\nu(\mathrm{z} + d_\mathrm{z}, s + d_s), \tag{4.13}$$

and the *predicted reduction* (pred) is defined as

$$\mathrm{pred}(d) = q_\nu(0) - q_\nu(d), \tag{4.14}$$

where q_ν is defined as

$$q_\nu(d) = (\nabla\mathscr{B})^\top d + \frac{\sigma}{2}\left(d_\mathrm{z}^\top \nabla^2_{\mathrm{zz}}\mathscr{L} d_\mathrm{z} + \mu d_s^\top S^{-2} d_s\right) + \nu m(d),$$

with

$$m(d) = \|A(\mathrm{Z})d_{\mathrm{Z}} - d_s + g(\mathrm{Z}) - s\| - \|g(\mathrm{Z}) - s\| \text{ and } \sigma = \begin{cases} 1 & \text{if } d_z^\top \nabla^2_{\mathrm{ZZ}} \mathscr{L} d_z > 0, \\ 0 & \text{otherwise.} \end{cases}$$

To determine an appropriate value of the penalty parameter ν, we require that ν be large enough that satisfies the following inequality for some $\rho \in (0,1)$:

$$\mathrm{pred}(d) \geq \rho \nu \left(m(0) - m(d) \right). \tag{4.15}$$

The inequality (4.15) provides the minimum value of the penalty parameter ν. Therefore, the minimum value of the penalty parameter is determined as follows:

$$\nu_{\min} = \frac{(\nabla \mathscr{B})^\top d + \frac{\sigma}{2} \left(d_{\mathrm{Z}}^\top \nabla^2_{\mathrm{ZZ}} \mathscr{L} d_{\mathrm{Z}} + \mu d_s^\top S^{-2} d_s \right)}{(1-\rho) \|g(\mathrm{Z}) - s\|}. \tag{4.16}$$

In the proposed method, we typically choose $\nu = 2\nu_{\min}$.

The following theorem ensures that the step d is descent direction for the merit function ϕ_ν.

Theorem 4.2. *Consider barrier problem (4.2). Let the point $\Omega = (\mathrm{Z}, s, y)$ be such that $s > 0$ and $y > 0$. Assume that $\mathscr{L}$, for (4.2), is positive definite. Then, for any $\mu > 0$ and $\nu > \nu_{\min}$ (see (4.16)), the step d that is computed by solving the problem (4.4) is a descent direction for the merit function ϕ_ν.*

Proof. Since $\nu > \nu_{\min}$, from (4.16), we obtain the following inequality:

$$\nu > \frac{(\nabla \mathscr{B})^\top d + \frac{\sigma}{2} \left(d_{\mathrm{Z}}^\top \nabla^2_{\mathrm{ZZ}} \mathscr{L} d_{\mathrm{Z}} + \mu d_s^\top S^{-2} d_s \right)}{(1-\rho) \|g(\mathrm{Z}) - s\|}. \tag{4.17}$$

Note that $\nabla^2_{\mathrm{ZZ}} \mathscr{L}$ is positive definite and $\sigma \geq 0$. Therefore,

$$\frac{\sigma}{2} \left(d_{\mathrm{Z}}^\top \nabla^2_{\mathrm{ZZ}} \mathscr{L} d_{\mathrm{Z}} + \mu d_s^\top S^{-2} d_s \right) \geq 0.$$

Now, the inequality (4.17) can be written as

$$(\nabla \mathscr{B})^\top d - \nu \|g(\mathrm{Z}) - s\| < -\rho \nu \|g(\mathrm{Z}) - s\|. \tag{4.18}$$

Also, the directional derivative of the merit function ϕ_ν along the direction d is given by

$$\left(\nabla \phi_\nu(\lambda_\mu) \right)^\top d = (\nabla \mathscr{B})^\top d - \nu \|g(\mathrm{Z}) - s\|. \tag{4.19}$$

Since $\rho \in (0,1)$ and $\nu > 0$ then we obtain from (4.18) and (4.19) that

$$\left(\nabla \phi_\nu(\lambda_\mu) \right)^\top d \leq -\rho \nu \|g(\mathrm{Z}) - s\| < 0.$$

Hence, the result follows. □

The following algorithm provides a detailed step-wise procedure to find the nondominated points of MOPs with the help of the process described above. We use the following error function for the stopping criteria:

$$E(\mathrm{Z}, s, y) = \max \left\{ \|c - (A(\mathrm{Z}))^\top y\|, \|Sy - \mu e\|, \|g(\mathrm{Z}) - s\| \right\}. \tag{4.20}$$

Algorithm 1 Trust-region interior-point method for MOPs

Inputs:
(a) Give MOP (2.1)
(b) Provide the number of subproblems (N) to be solved

1: **Initialization:**
Set Pareto set $\mathscr{P} \leftarrow \emptyset$
Provide an initial point $w_0 = (\mathrm{z}_0, s_0, y_0) \in \mathbb{R}^{3n+2m+5p+8}$ with $\mathrm{z}_0 > 0,\ s_0 > 0$
Provide the initial trust region radius $\Delta_0 > 0$ and the constants $0 < \sigma < 1$, $\eta > 0$, $0 < \rho < 1$
Choose an initial value for $\mu > 0$
Give the accuracy precision $\varepsilon > 0$
Set $k \leftarrow 0$ (iteration number)

2: **Main Part:**
3: **for** $i = 1 : N$ **do**
4: Choose randomly $a \in \mathbb{R}^p, r \in \mathbb{R}^p \setminus \{0\}$ and $\omega \geq 0$
5: **while** $E(\mathrm{z}_k, s_k, y_k) \geq \varepsilon$ (see (4.20) for E) **do**
6: **while** $E(\mathrm{z}_k, s_k, y_k; \mu_k) \geq \mu$ **do**
7: Compute Lagrange multiplier y by solving the problem (4.9)
8: Compute $v_k = (v_\mathrm{z}, v_s)$ by solving (4.7)
9: Compute $\tilde{d}_k$ by applying the projected CG method to (4.6)
10: Obtain the total step d_k from (4.5)
11: Update v_k to satisfy (4.15)
12: Compute $\mathrm{pred}_k(d_k)$ by (4.14) and $\mathrm{ared}_k(d_k)$ by (4.13)
13: **if** $\mathrm{ared}_k(d_k) \geq \eta\, \mathrm{pred}_k(d_k)$ **then**
14: Set $\mathrm{z}_{k+1} \leftarrow \mathrm{z}_k + d_\mathrm{z},\ s_{k+1} \leftarrow s_k + d_s$
15: Choose $\Delta_{k+1} = 1.2\Delta_k$
16: **else**
17: Set $\mathrm{z}_{k+1} = \mathrm{z}_k,\ s_{k+1} = s_k$ and choose $\Delta_{k+1} = 0.8\Delta_k$
18: **end if**
19: $k \leftarrow k+1$
20: **end while**
21: Set $\mu \leftarrow \sigma\mu$
22: **end while**
23: Calculate $f(\mathrm{z})$
24: Update Pareto set $\mathscr{P} \leftarrow \mathscr{P} \bigcup \{f(\mathrm{z})\}$
25: **end for**
26: **return** The set $\mathscr{P}$ (a discrete approximation of the whole Pareto set)

4.3. **Well-definedness of Algorithm 1.** The well-definedness of Algorithm 1 depends on line numbers 8 and 9. Problem (4.7) is in the standard form of the trust-region problem if we neglect the constraint $\tilde{d}_s \geq -\tau e$ in problem (4.7). By reducing the value of the trust-region Δ, dogleg method solves the problem (4.7) for v until the constraint $\tilde{d}_s \geq -\tau e$ is satisfied. Hence, at the kth iteration, Algorithm 1 will be able to compute v_k. The vector v is a particular solution of the constraints of the problem (4.6). CG method is applied to solve the equally-constrained quadratic problem (4.6) for $\tilde{d}$ in Algorithm 1. Thus, Algorithm 1 will be able to compute $\tilde{d}_k$ and hence the total step d_k (see (4.5)) at kth iteration.

As an example, we consider the following bi-objective optimization problem:

$$\left.\begin{array}{ll}\text{minimize} & \left((x_1-1)^2+(x_1-x_2)^2,(x_1-x_2)^2+(x_2-3)^2\right)\\ \text{subject to} & 0\le x_1\le 5,\ 0\le x_2\le 5.\end{array}\right\} \tag{4.21}$$

The convergence of Algorithm 1 towards the Pareto points of the problem (4.21) is shown in FIGURE 1. To obtain a discrete approximation of Pareto front of the problem (4.21), Algorithm 1 solves the Pascoletti-Serafini scalar optimization problem with different values of $a\in\mathbb{R}^p_{\geqq}$, $r\in\mathbb{R}^p_{\geqq}-\{0\}$ and $\omega\ge 0$. We provide an initial point $w^{(0)}=(z^{(0)},s^{(0)},y^{(0)})$, where $z^{(0)}=(0.5,2,1,1)$, $y^{(0)}=s^{(0)}=(1,1,\dots,1)\in\mathbb{R}^{13}$, initial trust region radius $\Delta_0=0.3$ and initial value of $\mu=0.98$. Also, we choose $\sigma=0.95$, $\eta=0.8$, $\rho=0.75$ and the precision $\varepsilon=10^{-6}$. Algorithm 1 starts by choosing $a=(0,0)$, $r=(0.986,0.002)$ and $\omega=(1,1)$. The Algorithm 1 then computes $E(z_0,s_0,y_0)=317.809$ and checks the termination condition $E(z_0,s_0,y_0)>\varepsilon$. As this condition is true, it computes the Lagrange multiplier $y_0=10^{-3}$ by (4.9), and further computes the direction d_0. Thereafter, it increases or decreases the radius of trust region according to the condition (4.12). Algorithm 1 solves the barrier problem (4.2) for decreasing value of μ. Hence, Algorithm 1 gradually moves towards the solution of the barrier problem (4.2). After finding one efficient point, Algorithm 1 changes the value of a,r and ω and then converges to another efficient point. In a similar way, Algorithm 1 generates a set of efficient points by changing the values of a,r and ω. We solve the problem (4.21) by taking 50 different values of the parameters a,r and ω. We have shown all the iterations in the objective space (see FIGURE 1). The blue point $(2.5,3.25)$ in FIGURE 1 is the starting point in the objective space and violet points are the generated Pareto points corresponding to different values of a,r and ω. Note that the initial point remains unchanged throughout the entire process (see FIGURE 1).

In the next section, we apply Algorithm 1 to some standard test problems and solve a tuberculosis optimal control problem.

5. Numerical Results and Applications

This subsection reports outcomes of the applications of the proposed TR-IPM on several test problems (see Table 1) found in the literature. The test was carried out on a PC with Intel Core i7-4770U 3.40 GHz CPU and 4GB RAM in MATLAB 2020a. The Pareto front of these problems are shown in red color and obtained Pareto points by Algorithm 1 shown in blue colour (see FIGURE 2). The graphs in FIGURE 2 show that the proposed algorithm can efficiently achieve convex, nonconvex, connected, and disconnected Pareto fronts.

6. Optimal Control of a Tuberculosis Model

This section provides an application of optimal control strategies in a tuberculosis (TB) model which is taken from [20]. The model is a system of ordinary differential equations which considers reinfection and post-exposure interventions. In the model, the population is divided into the following five categories:

- S represents the susceptible population;
- L_1 indicates the early latent population, i.e., a person who is recently infected for not more than two years but not infectious;
- I indicates the infected population which has active tuberculosis and is infectious;
- L_2 indicates the persistent latent population, i.e., the number of individuals who are infected and latent;
- R indicates the recovered population, i.e., the number of individuals who are previously infected and treated.

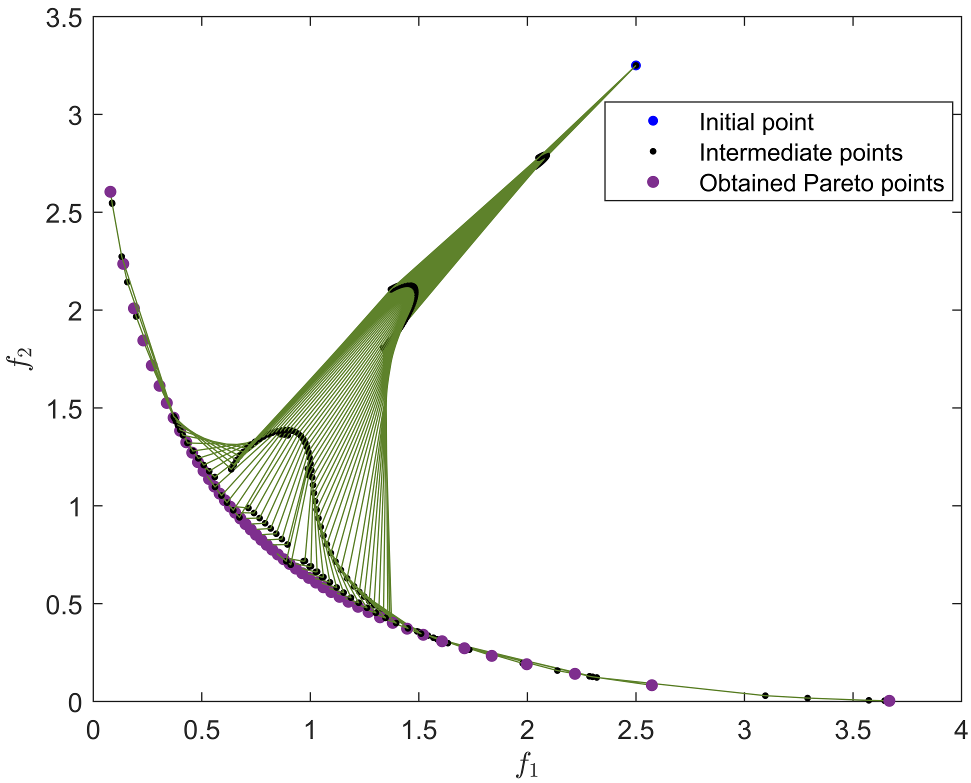

FIGURE 1. Obtained Pareto points of the example (4.21) by Algorithm 1
.

TABLE 1. Data for the test problems

Problem name	n	Nondominated set type	Variables' domain
SCH [25]	1	Convex	$[-1000, 1000]$
FON [26]	10	Nonconvex	$[-4, 4]$
ZDT1 [27]	10	Convex	$[0, 1]$
ZDT2 [27]	10	Nonconvex	$[0, 1]$
ZDT3 [27]	10	Nonconvex and disconnected	$[0, 1]$
ZDT4 [27]	10	Convex	$[0, 1]$
DTLZ1 [25]	10	Convex	$[0, 1]$
DTLZ2 [25]	10	Nonconvex	$[0, 1]$

It is assumed that the total population $N = S + L_1 + I + L_2 + R$ is constant. The control variable of the model system are as follows:

- $v_1(t)$ is a measurement representative that represents the measures taken to prevent treatment failure in active TB infected individuals I, such as following up with patients and helping them to take their prescribed medication and completing the treatment regimen.

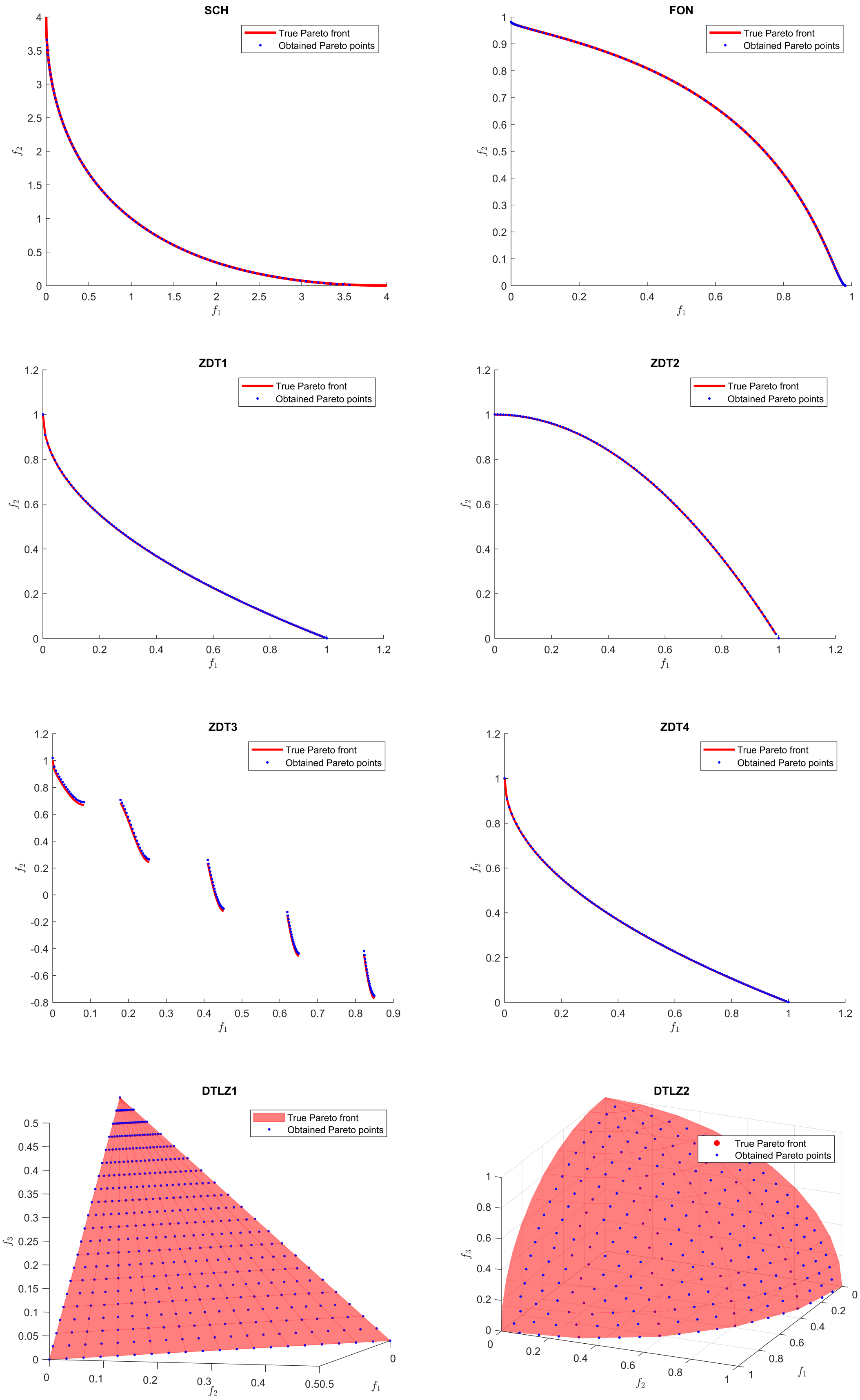

FIGURE 2. Obtained Pareto points vs true Pareto front.

- $v_2(t)$ represents the fraction of persistent latent individuals who have been identified and put under treatment.

According to Denysiuk et al. [20], the tuberculosis is modelled by the following system of nonlinear time-varying state equations with $v_1(t)$ and $v_2(t)$ as their control variable:

$$\begin{cases} \dot{S} = \mu N - \frac{\beta}{N} IS - \mu S, \\ \dot{L_1} = \frac{\beta}{N} I(S + \sigma L_2 + \sigma_R R) - (\sigma + \tau_1 + \mu) L_1, \\ \dot{I} = \phi \sigma L_1 + \omega L_2 + \omega_R R(t) - (\tau_0 + \varepsilon_1 v_1(t) + \mu) I, \\ \dot{L_2} = (1 - \phi)\delta L_1 - \sigma \frac{\beta}{N} I L_2 - (\omega + \varepsilon_2 v_2(t) + \tau_2 + \mu) L_2, \\ \dot{R} = (\tau_0 + \varepsilon v_1(t)) I + \tau_1 L_1 + (\tau_2 + \varepsilon_2 v_2(t)) L_2 - \sigma_R \frac{\beta}{N} IR - (\omega_R + \mu) R, \end{cases} \tag{6.1}$$

with the initial conditions

$$S(0) = \frac{76}{120} N,\ L_1(0) = \frac{37}{120} N,\ I(0) = \frac{4}{120} N,\ L_2(0) = \frac{2}{120} \text{ and } N,\ R(0) = \frac{1}{120} N, \tag{6.2}$$

where the parameters in the system (6.1) are provided in the following table:

Symbols	Description	Value
β	Transmission coefficient	75, 100, 125
μ	Death and birth rate	1/70 yr^{-1}
δ	Rate at which individuals leaves L_1	12 yr^{-1}
ϕ	Proportion of the individuals going to I	0.05
ω	Rate of endogenous reactivation for persistent latent infections	0.0002 yr^{-1}
ω_R	Rate of endogenous reactivation for treated individuals	0.00002 yr^{-1}
σ	Factor reducing the risk of infection as a result of acquired immunity to a previous infection for L_2	0.25
σ_R	Rate of exogenous reinfection of treated patients	0.25
τ_o	Rate of recovery under treatment of active TB	2 yr^{-1}
τ_1	Rate of recovery under treatment of latent individuals L_1	2 yr^{-1}
τ_2	Rate of recovery under treatment of latent individuals L_2	1 yr^{-1}
N	Total population	30,000
ε_1	Efficacy of treatment of active TB I	0.25
ε_2	Efficacy of treatment of active TB L_2	0.25
T	Total simulation duration	5 yr

TABLE 2. Description and values of the parameters in the model problem (6.7)

We obtain the values of parameters used in model system (6.1) from [20] and the references cited therein.

Styblo [28] indicated that disease risk after infection is highest in the first five years and then declines exponentially. In the view of this, we consider the total simulation duration of $T = 5$ years.

6.1. **Optimal control problem formulation.** Our aim is to determine the optimal values v_1^* and v_2^* of the controls v_1 and v_2 such that (i) the corresponding state trajectories S^*, L_1^* I^*, L_2^* and R^* are the solution of the system (6.1) and (6.2), in the time interval $[0,T]$ and (ii) minimize the following objective functional:

$$J(v_1, v_2) = \int_0^T \left[I(t) + L_2(t) + w_1 v_1^2(t) + w_2 v_2^2(t) \right] dt. \tag{6.3}$$

Here, the objective functional involves the number of active TB infectious individuals I, the number of persistent latent individuals L_2, and the implementation cost of the strategies associated with the controls v_1 and v_2. The controls are bounded by 0 and 1. When the controls vanish, no extra measures are implemented for the reduction of I and L_2; when the controls take the maximum value 1, the magnitude of the implemented measures associated to v_1 and v_2 take the values ε_1 and ε_2, respectively.

Consider the model system of ordinary differential equations (6.1). Suppose the set of permissible control functions is given by the following Lebesgue measurable set

$$\Psi = \{(v_1, v_2) : 0 \le v_1(t), v_2(t) \le 1,\ \forall t \in [0, T]\}.$$

Hence, the proposed problem is to minimize the objective functional (6.3), where the constants w_1 and w_2 give relative cost of the interventions associated to the control v_1 and v_2, respectively. The following problem

$$J(v_1^*, v_2^*) = \min_{(v_1,v_2)\in\Psi} J(v_1, v_2) \tag{6.4}$$

has two main aspects: (i) minimizing the number of active infected and latent individuals and (ii) reducing the implementation cost of control policies.

6.2. **Multi-objective approach to the optimal control problem (6.4).** The available approaches that use the idea of optimal control theory have a significant disadvantage that it can only yield a single optimal solution for the problem (6.4). The determination of a single optimal requires decision-maker's preferences involving a pair of weight constants w_1 and w_2; see [20, 29] for details and the references therein. However, the choice of parameters w_1 and w_2 is not straightforward. It requires some prior knowledge about the problem and decision maker's preferences, which may not always be available. Nevertheless, single optimal solution for the problem (6.4) does not provide all helpful insights for the optimal strategies and for the corresponding dynamics. Thus many optimal alternatives remains unexplored by using the approaches based on optimal control theory.

The current work proposes an approach that uses the idea of multi-objective optimization, which may provide the Pareto solutions instead of a single optimal solution. In the proposed approach, we decompose the cost functional (6.3) into two components f_1 and f_2, where

$$f_1(v_1, v_2) = \int_0^T \big[I(t) + L_2(t)\big]\,dt \text{ and} \tag{6.5}$$

$$f_2(v_1, v_2) = \int_0^T \big(v_1^2(t) + v_2^2(t)\big)\,dt. \tag{6.6}$$

Thus a bi-objective formulation corresponding to (6.4) can be defined by the following:

$$\left.\begin{aligned}
&\text{minimize} && (f_1, f_2)\\
&\text{subject to} && \dot{S} = \mu N - \frac{\beta}{N} IS - \mu S,\\
& && \dot{L_1} = \frac{\beta}{N} I(S + \sigma L_2 + \sigma_R R) - (\sigma + \tau_1 + \mu)L_1,\\
& && \dot{I} = \phi\sigma L_1 + \omega L_2 + \omega_R R(t) - (\tau_0 + \varepsilon_1 v_1(t) + \mu)I,\\
& && \dot{L_2} = (1-\phi)\delta L_1 - \sigma\frac{\beta}{N} IL_2 - (\omega + \varepsilon_2 v_2(t) + \tau_2 + \mu)L_2,\\
& && \dot{R} = (\tau_0 + \varepsilon v_1(t))I + \tau_1 L_1 + (\tau_2 + \varepsilon_2 v_2(t))L_2 - \sigma_R\frac{\beta}{N} IR - (\omega_R + \mu)R,\\
& && S(0) = \frac{76}{120}N,\ L_1(0) = \frac{37}{120}N,\ I(0) = \frac{4}{120}N,\ L_2(0) = \frac{2}{120}N,\ R(0) = \frac{1}{120}N,\\
& && 0 \le v_1 \le 1,\\
& && 0 \le v_2 \le 1.
\end{aligned}\right\} \tag{6.7}$$

Note that f_1 represents the number of active infected and latent individuals during the period $[0,T]$, and f_2 represents the cost associated to the implementation of control policies during the period $[0,T]$. In the above formulation, the constants w_1 and w_2 are ignored.

6.3. **Algorithm.** The following Algorithm 2 describes a complete procedure to obtain the Pareto set corresponding to the bi-objective optimal control problem (6.7). We first numerically integrate the model system (6.1) by using the fourth-order Runge-Kutta method on the interval $[0,T]$, where $T = 5$ years. We discretize the range of the controls v_1 and v_2 on 80 equally spaced time intervals. Then, the integrals in (6.5) and (6.6) are calculated by applying the trapezoidal rule. Further, using Algorithm 1 we find a discrete approximation of complete Pareto set of the problem (6.7).

Algorithm 2 Algorithm to obtain the Pareto set of the optimal control problem (6.7).

1: Compute the numerical integration of the system (6.1) by using the fourth-order Runge-Kutta method on the interval $[0,T]$.
2: Discretize the control v_1 and v_2 on a set of equally spaced time intervals.
3: Compute the integrals in (6.5) and (6.6) by applying the trapezoidal rule in order to obtain the discrete approximation of f_1 and f_2.
4: Compute a quadratic approximation of f_1 and f_2 with the help of curve fitting.
5: Apply Algorithm 1 for the bi-objective optimization problem (f_1, f_2) subject to $0 \le v_1 \le 1$, $0 \le v_2 \le 1$ to find the discrete approximation of complete Pareto set.

6.4. **Numerical results.** In the following section, we present and analyze the numerical results obtained by applying Algorithm 2 on the model system (6.1). The parameter values for the problem (6.1) are taken from Table 2.

In the following part, we describe the obtained optimal solutions to the problem (6.7), taking into account the variations of the parameter β (transmission coefficient).

FIGURE 3 plots the criterion feasible region of the problem (6.7) for $\beta = 75, 100$ and 125.

FIGURE 4 plots the trade-off solution obtained for three different values of transmission coefficient β. From the figure, we observe that higher β values indicate higher level of infectious and persistent latent individuals is. Also, the difference between the worst and best case scenarios from medical perspective becomes large if β is increased.

In order to find the total number of active infected and latent individuals which are concentrated during the time span of 5 years we plot FIGURE 5. The figure depicts the values of f_1 as a function of Pareto optimal control strategy v_1^*, v_2^* for two different values of β. From FIGURE 5, we observe that the minimum and maximum values of f_1 increase as we increase the value of β.

7. Conclusion

In this paper, multi-objective optimization problems were solved with the help of Pascoletti-Serafini scalarization technique and interior point method. The Pascoletti-Serafini scalarization was used to transform an MOP into a set of scalar optimization subproblems. Thereafter, these subproblems were solved with the help of trust region interior point technique. The performance of Algorithm 1 was tested on some standard test problems. The results in Section 5 was shown the efficiency of Algorithm 1.

As an application, we applied the proposed Algorithm to solve a model problem for tuberculosis from optimal control view point, using a multi-objective approach. The optimal control strategies were determined by simultaneously minimizing the number of individuals infected with tuberculosis and the cost of implementing prevention and treatment policies. Using the proposed approach, additional weight coefficients were not needed in order to formulate a single cost functional. The results

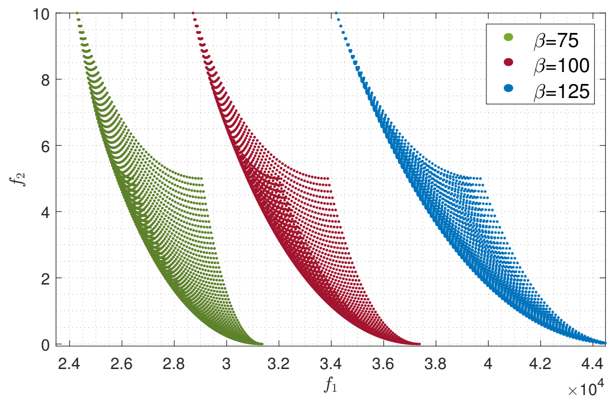

FIGURE 3. Feasible criterion region for different β's

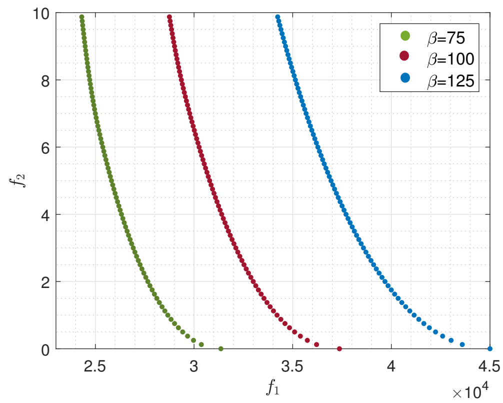

FIGURE 4. Trade-off curve for different values of β

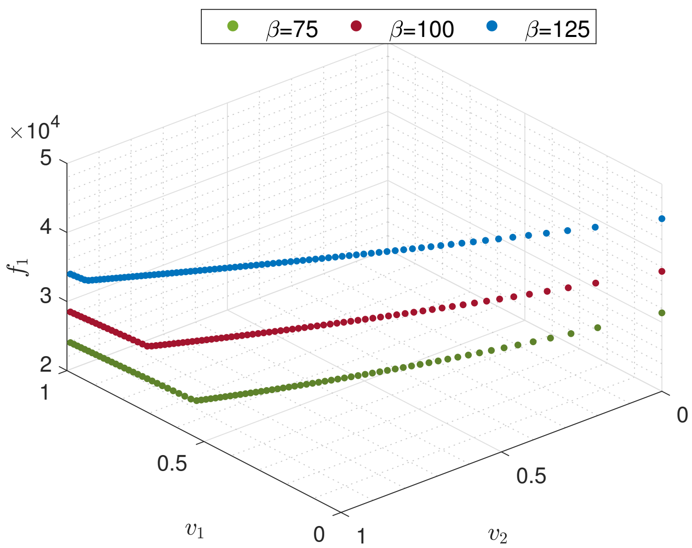

FIGURE 5. Representation of f_1 as a function of Pareto optimal strategies v_1 and v_2 for different values of β

of this study demonstrated how a comprehensive multi-objective approach can effectively identify the best control strategies within a mathematical model for tuberculosis. We found alternative viewpoints on implementing prevention and treatment policies using the obtained trade-off solutions. We analyzed the optimal control strategies with varying β (transmission coefficient). The obtained results depicted that as the transmission coefficient increases the proportion of active infectious and persistent latent individuals also increases. Furthermore, we observed that the maximum and minimum values of f_1 increase with the increase of transmission coefficient β.

Acknowledgments

D. Ghosh is thankful to the financial support of the research project grant MATRICS (MTR/2021/000696) by Science and Engineering Research Board, India. Jauny thankfully acknowledges financial support from Council of Scientific and Industrial Research, India through a research fellowship (File No. 09/1217 (0025)/2017-EMR-I) to carry out this research work.

REFERENCES

[1] J. Andersson, Multiobjective optimization in engineering design: Applications to fluid power systems, Ph.D. Thesis, Linköpings Universitet, 2001.
[2] Y. Jin, B. Sendhoff, Pareto-based multiobjective machine learning: An overview and case studies, IEEE Trans. Syst. Man Cybern. Part C Appl. Rev. 38 (2008), 397-415.
[3] S. Peitz, Exploiting structure in multiobjective optimization and optimal control, Ph.D. Thesis, Universität Paderborn, 2017.
[4] G. P. Rangaiah, A. B. Petriciolet, Multi-objective optimization in chemical engineering: Developments and Applications, John Wiley & Sons, 2013.
[5] X. Zhao, L. O. Jolaoso, Y. Shehu, J. C. Yao, Convergence of a nonmonotone projected gradient method for nonconvex multiobjective optimization, J. Nonlinear Var. Anal. 5 (2021), 441-457.
[6] K.D. Bae, Z. Hong, D.S. Kim, A minimax approach to characterize quasi ε-Pareto solutions in multiobjective optimization problems, J. Nonlinear Var. Anal. 5 (2021), 709-720.
[7] M. Ehrgott, Multicriteria optimization, Second Edition, Springer-Verlag, Berlin Heidelberg, 2005.
[8] R.T. Marler, J.S. Arora, Survey of multi-objective optimization methods for engineering, Struct. Multidiscipl. Optim. 26 (2004), 369-395.
[9] A. Pascoletti, P. Serafini, Scalarizing vector optimization problems, J. Optim. Theory Appl. 42 (1984), 499-524.
[10] G. Eichfelder, Adaptive Scalarization Methods in Multiobjective Optimization, Springer, Berlin, 2008.
[11] I.Y. Kim, O.L. de Weck, Adaptive weighted-sum method for bi-objective optimization: Pareto front generation, Struct. Multidiscip. Optim. 29 (2005), 149-158.
[12] R.T. Marler, J.S. Arora, The weighted sum method for multi-objective optimization: New insights, Struct. Multidiscipl. Optim. 41 (2010), 853-862.
[13] K. Khalili-Damghani, M. Amiri, Solving binary-state multi-objective reliability redundancy allocation series-parallel problem using efficient epsilon-constraint, multi-start partial bound enumeration algorithm, and DEA, Reliab. Eng. Syst. 103 (2012), 35-44.
[14] I. Das, J.E. Dennis, Normal-boundary intersection: A new method for generating the Pareto surface in nonlinear multicriteria optimization problems, SIAM J. Optim. 8 (1998), 631-657.
[15] D. Ghosh, D. Chakraborty, A new nondominated set generating method for multi-criteria optimization problems, Oper. Res. Lett. 42 (2014), 514-521.
[16] F. Akbari, M. Ghaznavi, E. Khorram, A revised pascoletti–serafini scalarization method for multiobjective optimization problems, J. Optim. Theory Appl. 178 (2018), 560-590.
[17] N. Karmarkar, A new polynomial-time algorithm for linear programming, Combinatorica 4 (1984), 373-395.
[18] B. El-Sobky, An interior-point penalty active-set trust-region algorithm, J. Egyptian Math. Soc. 24 (2016), 672-680.
[19] B. El-Sobky, A global convergence theory for an active-trust-region algorithm for solving the general nonlinear programing problem, Appl. Math. Comput. 144 (2003), 127-157.
[20] R. Denysiuk, C. J. Silva, D. F. Torres, Multiobjective approach to optimal control for a tuberculosis model, Optim. Meth. Softw. 30 (2015), 893-910.
[21] R. Fletcher, Practical methods of optimization, John Wiley & Sons, 2013.
[22] J. Nocedal, S. Wright, Numerical optimization, Springer Science & Business Media, 2006.
[23] J. E. Dennis Jr, M. El-Alem, K. Williamson, A trust-region approach to nonlinear systems of equalities and inequalities, SIAM J. Optim. 9 (1999), 291-315.

[24] T. Steihaug, The conjugate gradient method and trust regions in large scale optimization, SIAM J. Numer. Anal. 20 (1983), 626–637.

[25] K. Deb, L. Thiele, M., Laumanns, E. Zitzler, Scalable test problems for evolutionary multiobjective optimization, In: Abraham, A., Jain, L., Goldberg, R. (eds) Evolutionary Multiobjective Optimization. pp. 105–145, Springer, London, 2005.

[26] C. M. Fonseca, P. J. Fleming, Multiobjective optimization and multiple constraint handling with evolutionary algorithms. II. Application example, IEEE Trans. Syst. Man Cybern. Syst. 28 (1998), 38-47.

[27] E. Zitzler, K. Deb, L. Thiele, Comparison of multiobjective evolutionary algorithms: empirical results, Evol. Comput. 8 (2000), 173-195.

[28] K. Styblo, Epidemiology of Tuberculosis: Epidemiology of Tuberculosis in HIV Prevalent Countries, Royal Netherlands Tuberculosis Association, The Hague, 1991.

[29] R. Denysiuk, C.J. Silv, D.F. Torres, Multiobjective optimization to a TB-HIV/AIDS coinfection optimal control problem, Comput. Appl. Math. 37 (2018), 2112-2128.